We are IntechOpen,
the world's leading publisher of
Open Access books
Built by scientists, for scientists

6,900
Open access books available

185,000
International authors and editors

200M
Downloads

154
Countries delivered to

Our authors are among the

TOP 1%
most cited scientists

12.2%
Contributors from top 500 universities

CLARIVATE ANALYTICS
BOOK CITATION INDEX
INDEXED

WEB OF SCIENCE™

Selection of our books indexed in the Book Citation Index
in Web of Science™ Core Collection (BKCI)

Interested in publishing with us?
Contact book.department@intechopen.com

Recent Progress of Electrocatalysts and Photocatalysts Bearing First Row Transition Metal for Hydrogen Evolution Reaction (HER)

Shipra Sagar, Ravi K. Kanaparthi, Manish K. Tiwari and Satyen Saha

Abstract

The design and modification of metal–organic complexes for hydrogen (H_2) gas production by water splitting have been intensively investigated over the recent decades. In most reported mechanistic pathways, metal hydride species are considered as crucial intermediates for H_2 formation where the metal present at the active site plays an imperative role in the transfer of electron and proton. In the last few decades, much consideration has been done on the development of non-precious metal–organic catalysts that use solar energy to split water into hydrogen (H_2) and oxygen (O_2) as alternative fossil fuels. This review discussed the design, fabrication, and evaluation of the catalysts for electrocatalytic and photocatalytic hydrogen production. Mechanistic approach is addressed here in order to understand the fundamental design principle and structural properties relationship of electrocatalysts and photocatalysts. Finally, we discuss some challenges and opportunities of research in the near future in this promising area.
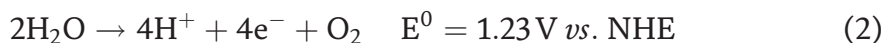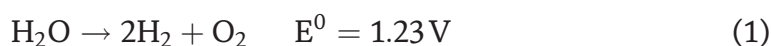
Keywords: redox-active-ligand, first-row transition metals, hydrogen evolution, catalytic cycle, electrocatalyst, photocatalyst

1. Introduction

Climate change and increasing energy demand have emphasized research on sustainable energy source [1, 2]. Day-by-day increase of human population and global requirements has compelled researchers to develop new renewable sustainable energy sources in replacement of hydrocarbon deposits [3]. Renewable sources such as solar power, wind, and water, storage of these energies for on-demand utilization, and transportation are the major challenges for researchers. To develop a clean and eco-friendly environment, splitting of water into hydrogen and oxygen is a tremendous way to produce sustainable energy. Hydrogen gas emerged as a green energy fuel due to its high-energy density and zero carbon dioxide (CO_2) emission [4–6]. In this regard, electrocatalytic and photocatalytic H_2 generation

from water has been considered as one of the most striking approaches [7–9]. In recent years, a substantial number of artificial photosynthesis have been developed, exploited solar power as electron and proton source to make a clean renewable fuel [10–14]. Light-induced splitting of water is a suitable process because the production of hydrogen is used as green fuel in future and even used for the synthesis of other chemicals [15–18].

Literature reports suggested more than 500 billion cubic meters (44.5 million tons) of hydrogen gas is produce yearly worldwide [19, 20]. In the current scenario, steam methane refining, coal gasification, and water electrolysis are the major way for hydrogen production. Nowadays 95% hydrogen gas is produced from steam methane reforming and coal gasification, however only 4% hydrogen from water electrolysis. Steam methane is a high-energy-intensive process maintained at high temperature with the formation of carbon dioxide and carbon monoxide: (i) $CH_4 + H_2O = CO + 3H_2$ (ii) $CO + H_2O = CO_2 + H_2$. Hence, it is not an eco-friendly method for hydrogen production. Water electrolysis is the most sustainable and clean approach for hydrogen production because its source is abundant. Since the most suitable way of light-driven energy conversion is water electrolysis, artificial photosynthesis (PS II) has been considered as primary goal to produce electron and proton [21, 22]. Water splitting is a redox reaction in which aqueous protons are reduced into H_2 at cathode and water is oxidized to O_2 at anode [23]. Both H_2 (HER) and O_2 (OER) reactions are rigorously coupled, which may lead to the formation of explosive H_2/O_2 mixtures due to gas crossover [24–26]. By far, only a few stable metal complexes as catalysts are achieved that can decompose water into H_2 and O_2 [27–31]. Water-splitting reactions are split into two half-reactions: water oxidation to O_2 evolution and water reduction to H_2 production:

$$H_2O \rightarrow 2H_2 + O_2 \quad E^0 = 1.23\,V \tag{1}$$

$$2H_2O \rightarrow 4H^+ + 4e^- + O_2 \quad E^0 = 1.23\,V \; vs. \; NHE \tag{2}$$

$$4H^+ + 4e^- \rightarrow 2H_2 \quad E^0 = 0\,V \; vs. \; NHE \tag{3}$$

The limitation of OER is that it takes place after the successive accumulation of four oxidized electrons and protons in Kok cycle (catalytic cycle of the water oxidation in PS II) that require much higher overpotential input than that of HER [32]. Thermodynamic potential is different for H^+/H_2 (0 V vs. NHE) and OH^-/O_2 (1.23 V vs. NHE), and the overall solar energy conversion efficiency is only ~15% in OER [33]. The hydrogen evolution reaction (HER, $2H^+ + 2e^- = H_2$) is the cathodic reaction with the two-electron transfer in one catalytic intermediate and offers the potential to hydrogen production. However, hydrogen production technology requires proficient electrocatalysts and photocatalysts which support two key electrode reactions (OER and HER) at lower overpotentials.

Moreover discussion on the mechanism of HER, H^+ adsorption on the hydrogen evolution catalyst surface is the first step, known as Volmer step, followed by Heyrovsky or Tafel steps shown in **Figure 1**. A suitable HER catalyst always binds H^+ very fast and releases the product. Hence, electrochemical hydrogen evolution reaction (HER) facilitates for H_2 production on large-scale.

Afterwards, H_2 evolution may occur via two different reaction mechanisms depending on the action of catalyst [34]. Hydronium cation (H_3O^+) is the proton source in acidic solution, and in alkaline condition H_2O is the proton source. In Volmer-Tafel mechanism, two protons absorbed on the catalytic surface can combine to form H-H bond to yield H_2. In Heyrovsky reaction route, a second electron and another proton from the solution are transferred to the catalyst surface which reacts with the absorbed H atom and generate H_2. This is an electrochemical
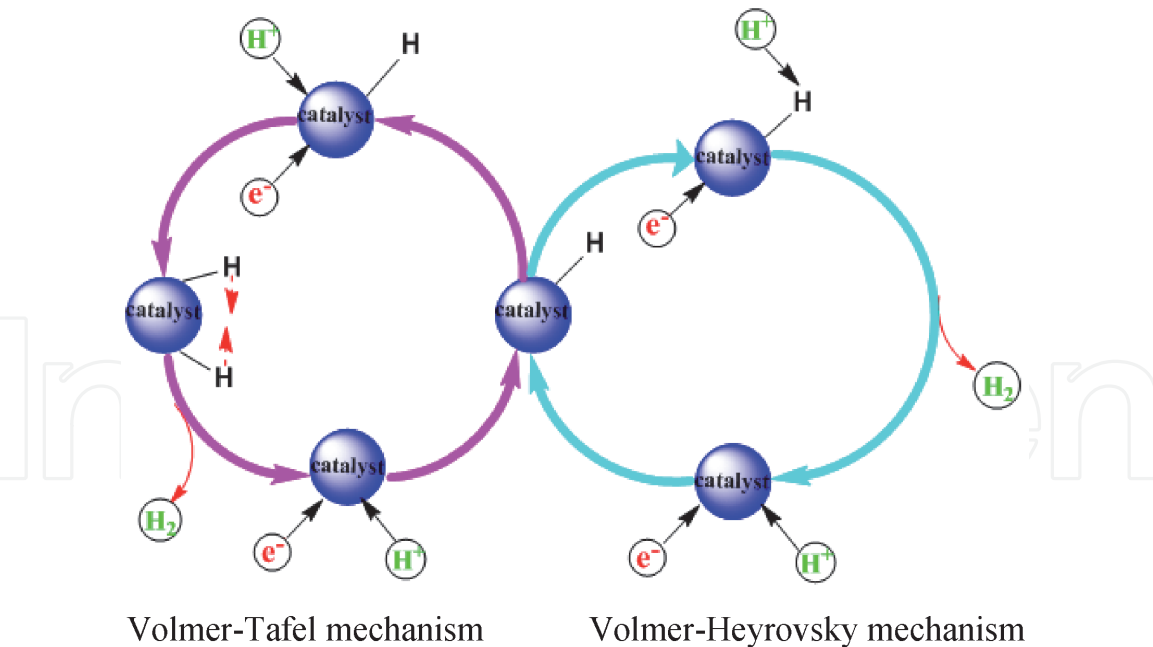
Figure 1.
The inside mechanism of H_2 evolution of electrocatalyst in acidic solution.

desorption pathway. Precious metal like Pt-based electrocatalysts is highly reactive for HER and is usually pursuing Volmer-Tafel mechanism. Lately few literatures [35–37] have been reported on Ni-based electrocatalysts which follows Volmer-Heyrovsky path.

1.1 Fundamental aspects of photocatalytic and electrocatalytic hydrogen production process

Electrocatalytic water splitting is driven by passing the electric current through the water; conversion of electrical energy to chemical energy takes place at electrode through charge transfer process. During this process, water reacts at the anode form O_2 and hydrogen (proton) produce at the cathode as we mentioned earlier. Suitable electrocatalysts can maximally reduce the overpotential which is highly desirable for driving a specific electrochemical reaction. However, the process of surface catalytic reactions in electrocatalysis is very similar to photocatalysis [38]. Photocatalytic is a simple water-splitting reaction in which H_2 and O_2 are produced from water by utilizing the energy of sunlight. **Figure 2(a)** shows the process of photocatalysis in which a metal catalyst contains chromophores that
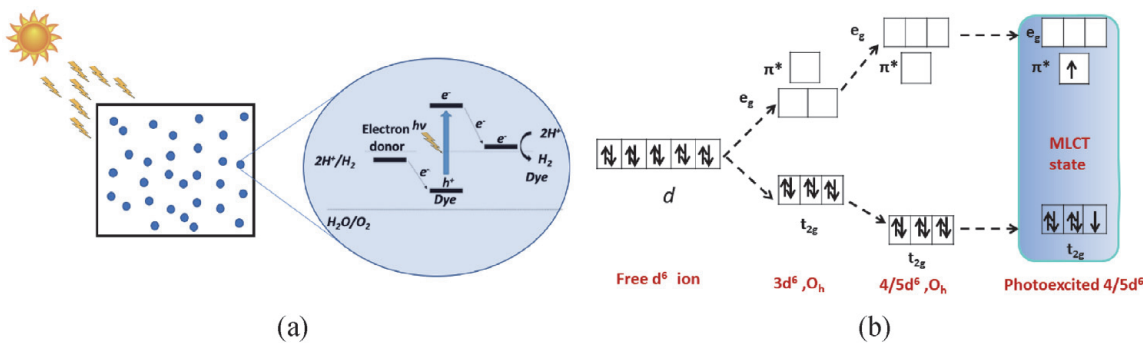

Figure 2.
(a) Photocatalyst system for water splitting. (b) Molecular orbital diagram for d^6 metal complex chromophores.

immersed solar energy and triggered the electron transfer reaction. The most important criteria for the solar-driven water-splitting reaction are electronic band gap matching of the photosensitive material to the redox potential of water [39]. Metal complexes act as chromophore associated with mainly three types of electron transfer: metal center (MC), ligand center (LC), and metal–ligand center transition (MLCT). The MLCT state of the metal complex plays a crucial role in photocatalytic reactions. In octahedral complexes with conjugated ligand system, the highest occupied molecular orbital (HOMO) corresponds to the metal-localized t_{2g}-orbitals, and the lowest unoccupied molecular orbital (LUMO) is associated with anti-bonding π^*-orbital localized on the ligands. On the absorption of UV–visible light, an electron is promoted from one of the metal-centered t_{2g} orbitals to a ligand-centered π^* orbital, resulting in the MLCT state shown in **Figure 2(b)**. As a result, the redox properties of the metal complexes are dramatically changed. The excited metal complexes behave as better oxidants and better reductants than their electronic ground state and can hold more thermodynamic driving force for the charge transfer reactions. Based on the photo-induced redox potential changes and the long-lived lifetime of the excited state, many metal complexes have been intensively investigated as chromophores for this photocatalytic H_2 production purpose [40]. Zou and coworkers have described various photocatalytic systems for H_2 production, which exposed that most of the photocatalytic systems suffer photodecomposition and instability [40]. Hence, for long-term use, it is imperative to build up highly proficient H_2 generation systems with long lifetimes and high durability. Many reviews have been published on solar H_2 evolution systems based on photocatalysts [41–44].

1.2 Mechanistic pathway

So far, extensive theoretical study has been revealed, the possible mechanistic process of proton reduction to hydrogen evolution through transition metal molecular catalyst. A generalized mechanistic scheme depicting the homolytic and heterolytic path is shown in **Figure 3**. The homolytic mechanism involves bimetallic route, where a metal hydride species ($[M^{n+}–H]$) react with another metal hydride to release one H_2 via reductive elimination. Instead, heterolytic is a monometallic
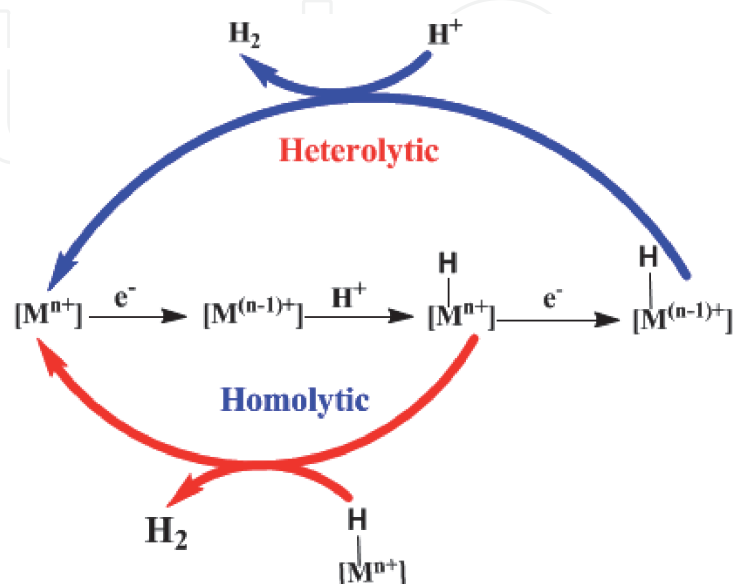

Figure 3.
Proposed homolytic and heterolytic mechanisms for H_2 evolution via the formation of a metal hydride (M-H) intermediate.

pathway, where the metal hydride [M^{n+}–H] is further reduce and protonated for H_2 evolution [45]. Both pathways function simultaneously, two protons and two electrons are delivered to the metal center, and in few cases, the pH, catalytic concentration, and proton source decide the dominant route [46]. During the past decade, a number of review articles emphases on the structural property relationship and mechanistic study [45, 47–49]. Among all research on catalyzed H_2 evolution, the mechanistic investigation on proton reduction catalysis is essential because it can give us a significant idea to design better molecular catalysts in the future [49].

1.3 Metal and redox-active ligands for HER

Here we start by describing the fundamental concept of metal and organic ligand system which gives a strong influence on the performance of H_2 evolution. Transition metal cations with partial filled d-electronic configurations are considered as catalyst. The characteristic feature of this type of catalyst is that the metal ions can exist in higher oxidation state [44]. There are several literatures reported with partially filled d-orbital which show high stability toward water-splitting reactions [50–53]. However, the most catalytic system requires very high temperature and precious metal at the active site; therefore, it will be a challenge for researchers to develop a photocatalytic and electrocatalytic system at low temperature with low-cost metal [54–57]. Indeed, first-row transition metal complexes (Co, Ni, Cu, Zn) have been exploited in the last few decades for this purpose. Beyond the reactivity of metal, the redox activity of organic ligands has also received continuous attention. The redox-active ligand works as electron sink in the complexes and maintains the metal in its original oxidation state. Redox-active ligands convey a novel reactivity to the complex by loss or gain of electrons [58]. In addition, the redox-active property of the ligand can also be influenced by the modification of the substituents by σ and π donating ability, π accepting ability, and conjugation [59]. A highly conjugated system such as bpy, porphyries, and ortho-phenylenediamine (opda) having anti-bonding π*-orbital localized on the ligands is considered for hydrogen production due to its multielectron or multiproton pooling ability which is responsible for dramatically changing the potential of redox properties [60, 61]. Substituents attached to redox-active ligands, electron density, and charge on the metal ions also effect the standard electrode potential.
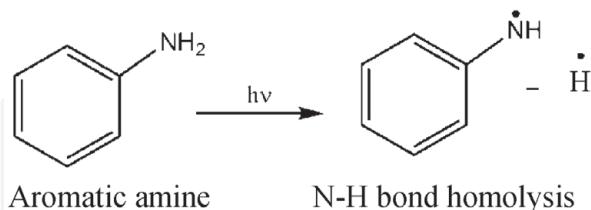
So far, considerable advancement has been done in the field of electrocatalytic and photocatalytic water-splitting reaction for hydrogen production, and several advance review papers have been reported by scientists [40, 51, 62–64]. However, very limited comprehensive tutorial has published on only first-row transition metal-based catalysts. This chapter describes electrocatalytic as well photocatalytic properties of inorganic catalysts and their structural and mechanistic features. Here we put an effort elucidate the direction of fundamental mechanistic aspects during electrocatalytic and photocatalytic hydrogen (H_2) production reaction (HER).

2. Photochemical hydrogen production from a series of 3D transition metal complexes bearing o-phenylenediamine ligand
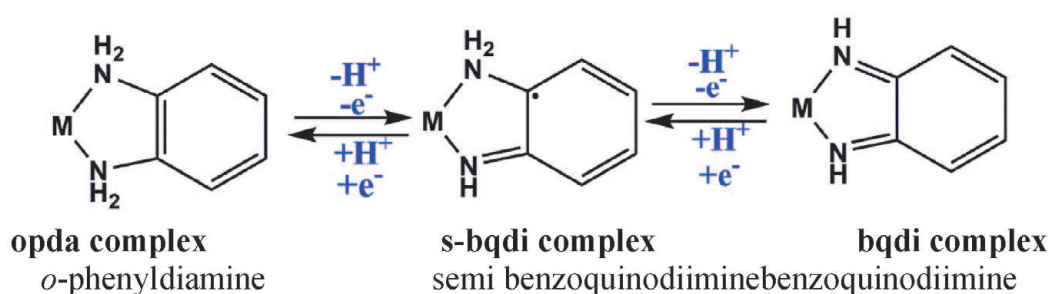
Masaki Yoshida et al. [65] developed a series of 3D-transition metal complexes with *o*- phenylenediamine (opda) ligands for hydrogen production due to the following properties: (**a**) aromatic amine undergoes homolytic N-H bond cleavage by photoexcitation [66] which is applicable for hydrogen production under mild condition, and (**b**) opda complexes have extensively been obsessed as reversible multielectron or multiproton pooling ability because of its multistep redox

processes between *o*-phenylenediamine(opda), semibenzoquinodiamine (s-bqdi), and *o*-benzoquinodiimine (bqdi) which is useful for reversible hydrogen production. [M(opda)$_3$], M = Mn^{2+}, Fe^{2+}, Co^{2+}, Ni^{2+}, and Zn^{+2} complexes (1–5) shown in **Table 1** have photochemical hydrogen production ability.

a. Photochemistry of aromatic amine (opda)

Aromatic amine   N-H bond homolysis

b. Redox properties of opda complex

opda complex   **s-bqdi complex**   **bqdi complex**
o-phenyldiamine   semi benzoquinodiiminebenzoquinodiimine
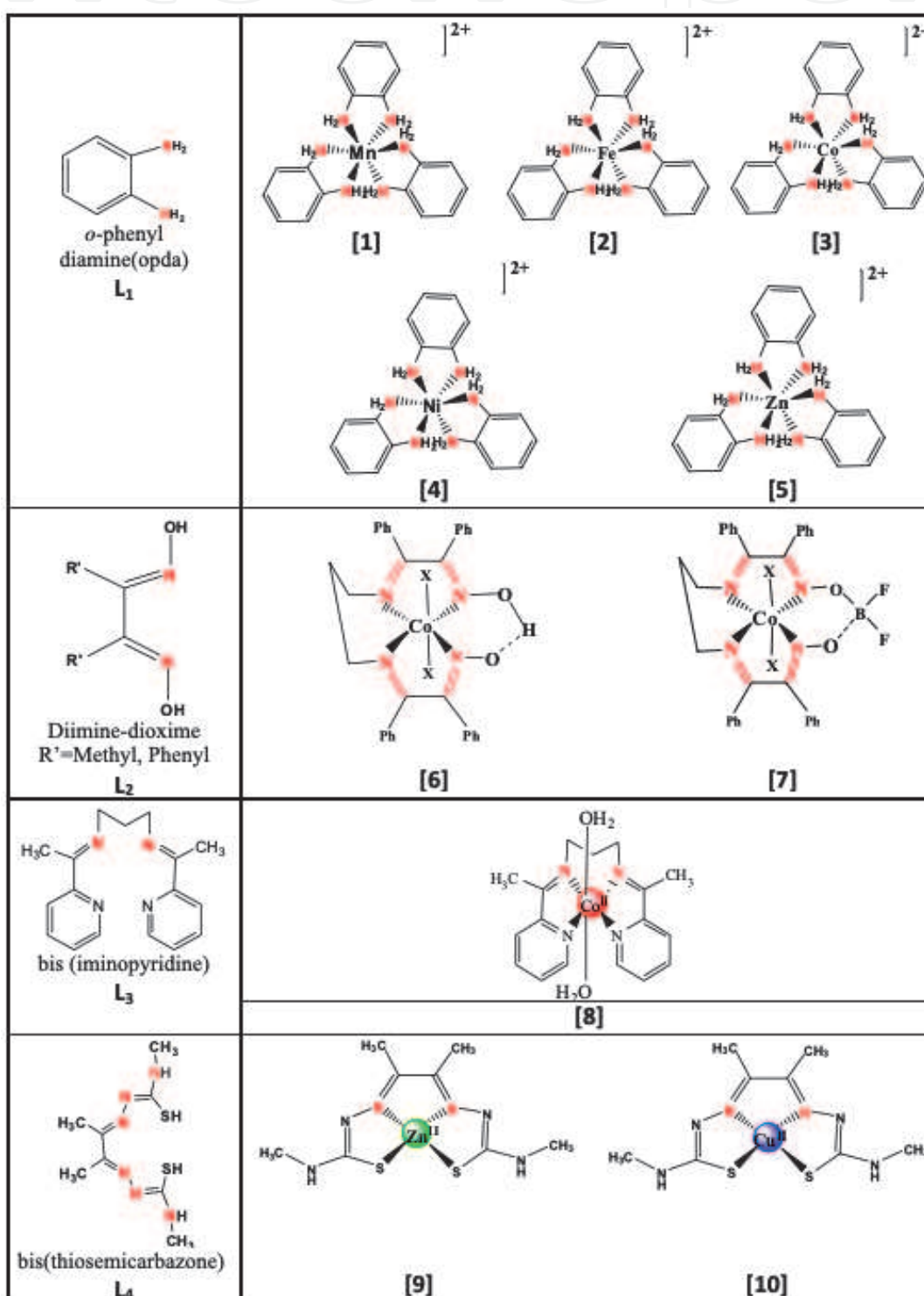
In the past M. Yoshida and coworkers proposed [Fe-opda] for photochemical HER mechanism at photoirradiation of λ = 298 nm; ππ* excitation occurred in complex with N-H bond homolysis process, followed by H$_2$ elimination [67]. After this process, the opda ligands in the complex were partially oxidized to bqdi or s-bqdi ligands. This mechanism is based on the deep-rooted photochemical N-H bond activation of aromatic amines. Theoretical study and ultrafast spectroscopic studies of amino benzene support that the photochemical N-H fission occurs by the photo-excitation to higher-lying ππ* level which leads to the formation of the πσ* state [68]. Photochemical mechanism for HER of all complexes is shown in **Figure 4**.

All opda-based metal complexes display photochemical HER activities with the formation of almost one equivalent of H$_2$ gas. However, the HER was not observed at all in the dark in all complexes, which suggests that the HER was obsessed by photochemical reaction. Moreover, they observed remarkable decrease in hydrogen evolution reaction, while the ligand is replaced with aromatic amines. This experiment suggested that the photo-induced HER activities of the complexes in this case are weakly dependent on the central metal ion and strongly dependent on the redox-active ligand. Further to check the metal ion dependency, examine the catalytic hydrogen production in the presence of hydroquinone (HQ; 10 equiv) as a sacrificial electron-proton donor. The photochemical H$_2$ production from [M-opda] (7.98×10^{-2} mmol) with HQ (7.98×10^{-1} mmol) in THF (4 mL) under an N$_2$ atmosphere at 20°C for 190 h turns over the number for all the complexes given in **Table 2**. Difference in TON may be caused by the stability of each complexes.

2.1 Cobalt diimine-dioxime complexes for HER

V. Artero and coworker synthesized cobalt diimine-dioxime complexes as molecular catalysts for H$_2$ evolution [69, 70]. This synthesized ligand (N^2, N^2_propanediylbis-butan-2-imine-3-oxime) has emerged many years ago through

Schiff base condensation of butanedione-monoximeon diamine compounds but not widely used for HER. Cobalt diimine-dioxime catalysts are active for H_2 evolution in aqueous solution, both after immobilization on electrode materials and in light-driven homogeneous conditions. The electrocatalytic activity of complexes (**6**) and (**7**) for hydrogen evolution was supported gas chromatography and by cyclic voltammetry study illustrated in **Figure 5** with the appearance of an irreversible wave. In the case of the BF_2-associated complex (**7**), the electrcatalytic wave which developed toward negative potentials corresponds to the Co^{II}/Co^{I} couple in contrast to the H-bridged complex (**6**), electrocatalytic H_2 evolution occurs at potentials positively shifted with regard to the Co^{II}/Co^{I} couple.
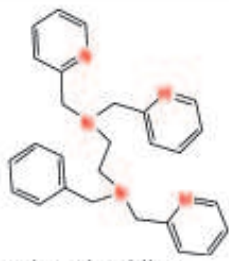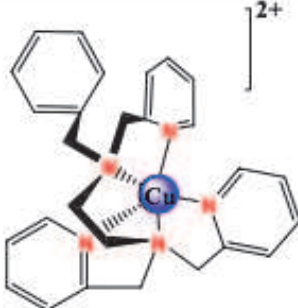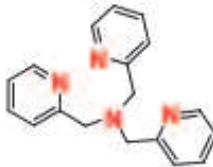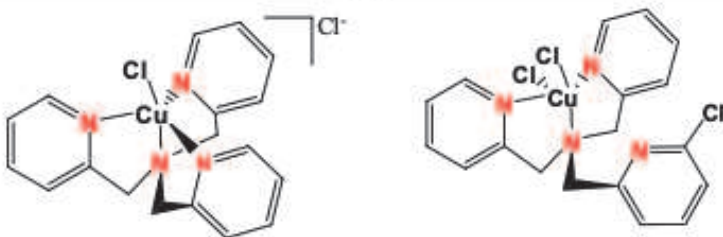
Table 1.
Structure of redox-active ligands, electrocatalysts, and photocatalysts.

$M^{II} = Mn^{+2}, Fe^{+2}, Co^{+2}, Ni^{+2}, Zn^{+2}$

Figure 4.
Plausible mechanism for photochemical HER with [M-opda] complexes.

2.2 Electrocatalytic cycle for H₂ evolution

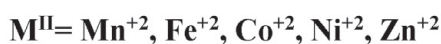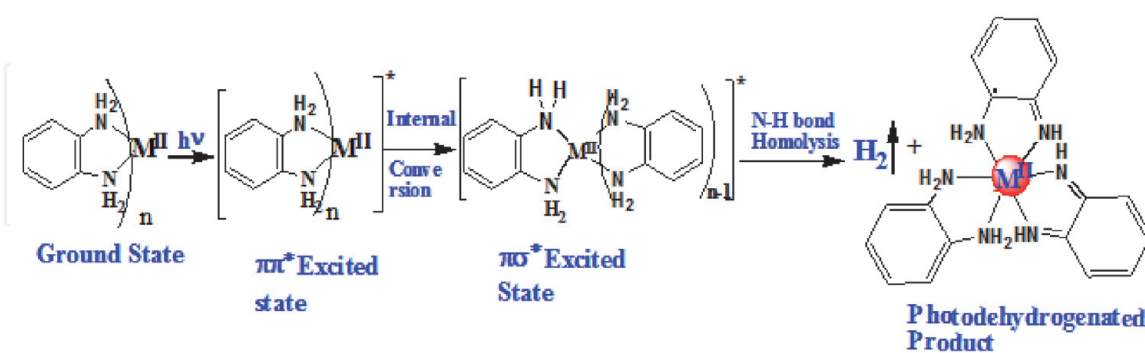In the electrocatalytic cycle, V. Artero and coworker observed that in acetonitrile medium, halide ligands are banished with reduced oxidation state from Co^{II} to Co^{I}. Upon reduction, the coordination in number decreases from six in Co^{II} state to

Catalysts	Redox-active organic ligands	Catalytic potential (Ep)	Solvent	TON(H$_2$ mol cat^{-1})	Ref.
[1][a]	o-Phenylenediamine	——	THF	5.5	[65]
[2]	o-Phenylenediamine	——	THF	2.9	[67]
[3]	o-Phenylenediamine	——	THF	0.99	[65]
[4]	o-Phenylenediamine	——	THF	0.51	[65]
[5]	o-Phenylenediamine	——	THF	0.73	[65]
[6][b]	Diimine-dioxime	-0.68 V vs. Fc$^{+/0}$	H$_2$O/CH$_3$CN	300	[70]
[7]	Diimine-dioxime	-0.96 V vs. Fc$^{+/0}$	H$_2$O/CH$_3$CN	50	[70]
[8]	Bis(thiosemicarbazone)	-1.7 V vs. Fc/Fc$^+$	CH$_3$CN	37	[74]
[9]	Bis(thiosemicarbazone)	-1.7 V vs. Fc/Fc$^+$	CH$_3$CN	73	[75]
[10][c]	Diamine-tripyridine	-0.90 V vs. Fc$^{+/0}$	acidic-H$_2$O	1.4x 10^4	[70]
[11][d]	TMPA	-1.81 V vs. SCE	CH$_3$CN/H$_2$O	6180	[76]
[12]	Cl-TMPA	-1.72 V vs. SCE	CH$_3$CN/H$_2$O	10,014	[76]
[13]	Bis(benzenedithiolate)	-2.25 V vs. SCE	CH$_3$CN	0	[77]
[14]	o-Aminobenzenethiolate	-1.64 V vs. SCE	CH$_3$CN	6190	[77]
[15]	o-Aminobenzene	-2.03 V vs. SCE	CH$_3$CN	900	[77]
[16]	2-Mercaptophenolate	-1.62 V vs. SCE	CH$_3$CN	5600	[77]

a = photochemical H$_2$ production from [M-opda 1–5] (7.98 × 10^{-2} mmol) with HQ (7.98 × 10^{-1} mmol) in (4 mL) under an N$_2$ atmosphere at 20°C for 190 h in the presence of 4 AMS (irradiation with 300 W Xe lamp, 250–385 nm). b = in light-driven condition of TEA and a cyclometalated iridium-based photosensitizer; CV was done in glassy carbon electrode (100 mVs^{-1}) in the presence of p-cyanoanilinium tetrafluoroborate. c = the controlled potential electrolysis of complex **11** was measured at pH 2.5 under N$_2$ atmosphere at a scan rate of 50 mVs^{-1}in phosphate buffer, over 2 hours using a glassy carbon electrode. d = conditions, 0.1 M n-Bu$_4$NPF$_6$, scan rate 100 mV/s, in Ar-saturated CH$_3$CN/H$_2$O.

Table 2.
Electrochemical data and catalytic efficiency of metal complexes for water-splitting hydrogen evolution reaction.
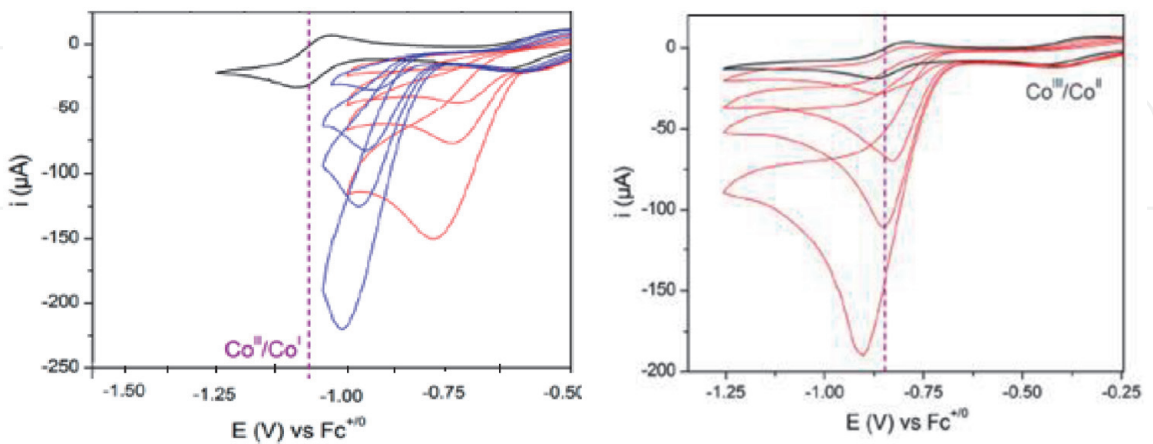

Figure 5.
Cyclic voltammograms of (6) Br$_2$ and (7) Br$_2$ (1 mM, black traces) recorded in CH$_3$CN at a glassy carbon electrode at a speed of 100 mV·s^{-1} (the figure is reproduced from Ref. [69], with permission from the publisher).

five in Co^I state; this characteristic was supported by DFT calculations [71]. In the catalytic cycle (**Figure 6**), the first step is the transfer of electron and proton by proton-coupled electron transfer (PCET) process. PCET is a chemical reaction that

involves the transfer of electron and proton in which the oxidation number changes by Co^{II} to Co^{I}. In the second steps, further electron and proton transfer takes place by PCET process, and the oxidation number changes from Co^{I} to Co^{II}. In the last step, H_2 is produced in dihydrogen bond through an intramolecular mechanism. The authors also confirmed cobalt diimine-dioxime catalysts **6** and **7** active for H_2 evolution under light-driven conditions in the presence of photosensitizers, associated with Ru, Ir, or Re derivatives. The photocatalytic activity of **6**-Br_2 was observed in mixed H_2O/CH_3CN solvent in the presence of TEA and cyclometalated iridium-based photosensitizer [72]. Turnover numbers (TON) determined after continuous 4 h UV–visible light irradiation **6**-Br_2 showed 300 (H_2 mol cat^{-1}), whereas **7**-Br_2 complex shows only 50 (H_2 mol cat^{-1}) as shown in **Table 2**.

Similarly, cobalt bis(iminopyridine) complex **8** was prepared for electrocatalytic water-splitting reaction [73]. The ligand-centered redox activity was observed during the cyclic voltammetry, suggesting the considerable role of redox-active ligand which is completely involved to stabilize the cobalt metal in higher oxidation state. The two reduction potentials were observed for the Co^{III}/Co^{II} (quasi reversible) and Co^{II}/Co^{I} (reversible) couples at -0.34 V and -0.86 V (vs. Ag/AgC), respectively. The improved water reduction was attributed to the assimilation of a redox-active-ligand to cobalt which facile reduction of $[Co-H]^{n+}$ species.

2.3 Zn^{II} and Cu^{II} complexes for HER

Grapperhaus et al. [74] recently reported two homogeneous electrocatalysts for H_2 production. They derived bis(thiosemicarbazones) ligand from 1,2-diones, considered as a kind of multitalented redox non-innocent system. Tetra-coordinated N_2S_2 is able to bind with low-valent transition metals centered and formed to stable neutral complexes (**9, 10**) (**Table 1**). Zn^{II} complex **9** containing a redox-active
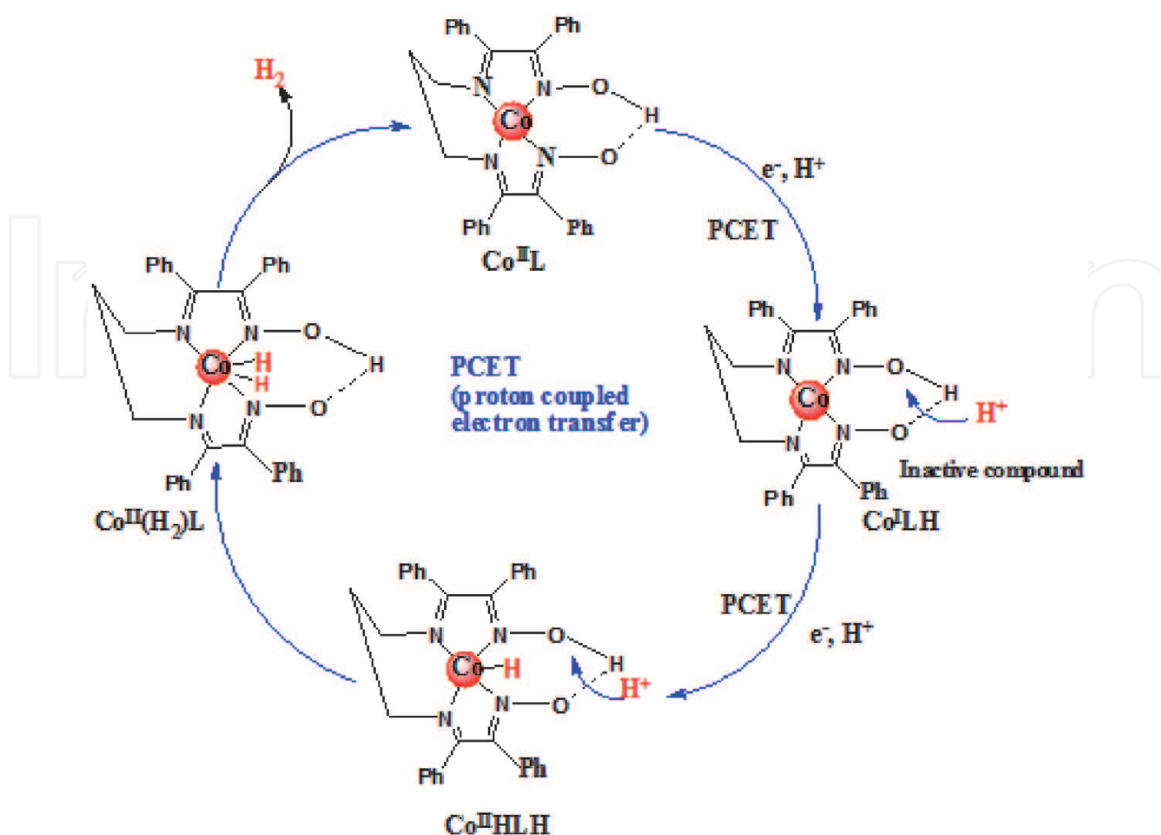

Figure 6.
Possible pathway for catalytic hydrogen evolution, involving PCET processes.

moiety diacetyl-bis (N-4 methyl-3-thiosemicarbazide) exhibits the homogeneous catalysis of electro-driven H_2 evolution through proton reduction with a maximum of TOF 1170 s^{-1} in CH_3OH and 11,700 s^{-1} in CH_3CN at an overpotential of 0.756 V and 1.074 V, CH_3COOH used as proton source. Bulk electrolysis showed that the TON of H_2 evolution of Zn^{II} is 37 in over 2.5 h experiments. To make this more comparative, Grapperhaus and coworker synthesized another Cu^{II} complex with similar ligand diacetyl-bis(N-4-methyl-3-thiosemicarbazide) and examined H_2 evolution reaction. Cu^{II} complex **10** exhibits a maximum TOF of 10,000 s^{-1} in CH_3CN and 5100 s^{-1} in DMF at an overpotential of 0.80 and 0.76 V, respectively. Controlled potential electrolysis confirmed Cu^{II} complex act as an excellent electrocatalyst to produce H_2 with a minimum faradic efficiency of 81% and TON as high as 73 during experiment over 23 h. They examined HER mechanism of complex **10** through DFT computational studies. In the proposed mechanism, initially the protonation occurs at the hydrazino nitrogen ligand. This was followed by an electrochemical step as a formation of reduced Cu^I species [Cu^I(HL)]. The second protonolysis occurs at the opposite hydrazine nitrogen of the ligand to yield [Cu^I(H$_2$L)]$^+$. Further one-electron reduction of [Cu^I(H$_2$L)]$^+$ leads to the formation of the H_2 evolution illustrated in **Figure 7**. Hence, here it is worth to mention that the identity of metal ions at the active site affects the HER mechanism.

Professor Wang and group proposed [75] a significant homogeneous mononuclear copper electrocatalyst for H_2 production attributed to diamine-tripyridine ligand; complex **11** attains trigonal bipyramidal geometry. According to the author, this ionic copper complex [Cu(bztpen)]$^{2+}$ with a five coordinating nitrogen atom shows a Jahn-Teller effect. Electrochemical and spectroscopic studies supported that the H_2 generation reaction takes place by two successive proton-coupled reduction processes. On the experimental observations of DPV, CV, UV–vis, and ^{1}H-NMR spectroscopic study, the authors proposed two possible pathways: path (A), protonation takes place at the Cu^I centered in the first step (Eqs. (4) and (5)), and path(B), protonation occurs at one of the nitrogen atoms of the ligand (Eqs. (6), (7), and (8)). H_2 generation reaction in path B takes place by two successive proton-coupled reduction processes. Protonation occurs at the ligand centered in the first reduction step, followed by the Cu^I centered in the second step. This provides [(bztpenH)Cu^{II}(H)]$^{2+}$ copper hydride species, which release H_2 and regenerate Cu^{II} catalyst.
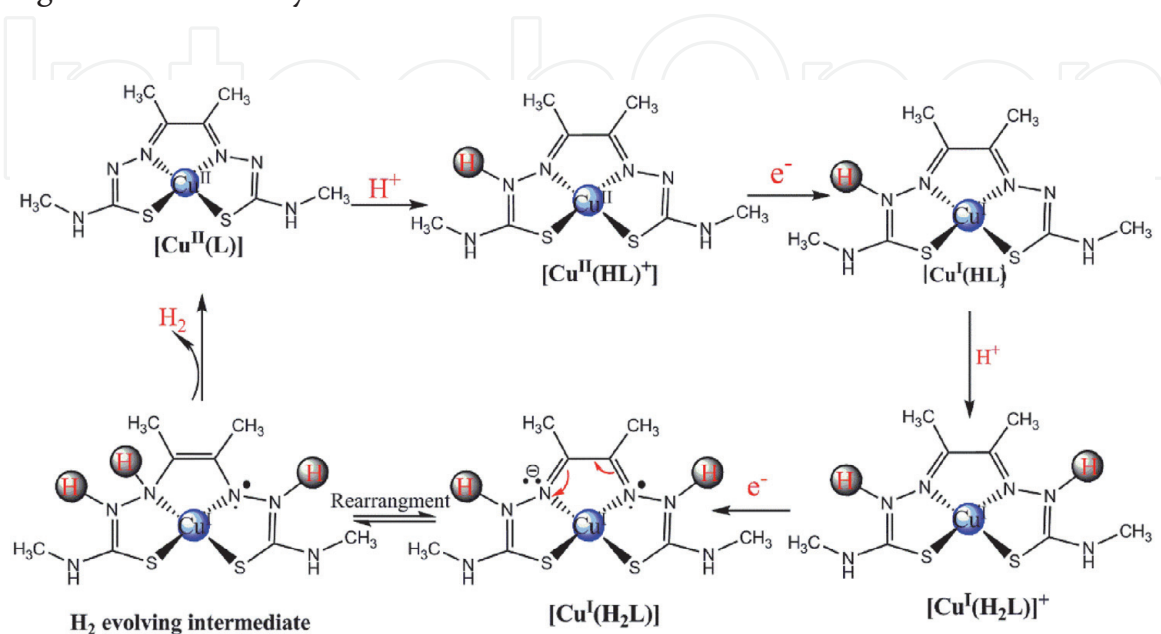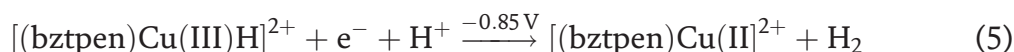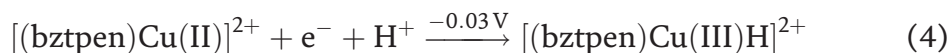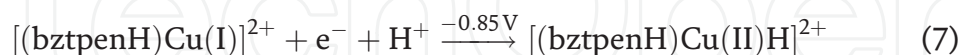

Figure 7.
Plausible mechanism for proton reduction in complex [CuL].

Path A:

$$[(bztpen)Cu(II)]^{2+} + e^- + H^+ \xrightarrow{-0.03\,V} [(bztpen)Cu(III)H]^{2+} \qquad (4)$$

$$[(bztpen)Cu(III)H]^{2+} + e^- + H^+ \xrightarrow{-0.85\,V} [(bztpen)Cu(II)^{2+} + H_2 \qquad (5)$$

Path B:

$$[(bztpen)Cu(II)]^{2+} + e^- + H^+ \xrightarrow{-0.03\,V} [(bztpenH)Cu(I)]^{2+} \qquad (6)$$

$$[(bztpenH)Cu(I)]^{2+} + e^- + H^+ \xrightarrow{-0.85\,V} [(bztpenH)Cu(II)H]^{2+} \qquad (7)$$

$$[(bztpenH)Cu(II)H]^{2+} \longrightarrow [(bztpen)Cu(II)]^{2+} + H_2 \qquad (8)$$
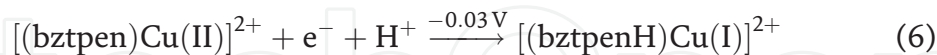
According to the author's studies on the mechanism of this process, the controlled potential electrolysis of complex **11** was measured at pH 2.5 in phosphate buffer at -0.90 V, over 2 h in a glassy carbon electrode. TON 1.4×10^4 mol H_2 (mol cat^{-1}) cm^{-2} was calculated on a faradic efficiency of approximately 96%, which corresponds to a TOF of 2.0 molH_2 (mol cat^{-1})s^{-1}cm^{-2}of $[(bztpen)Cu](BF_4)_2$.

Moreover, Wang et al. [76] fabricated and examined two Cu complexes with TMPA = tris(2-pyridyl)methylamine and Cl-TMPA 1-(6-chloropyridin-2-yl)methyl-*N*,*N*-bis(pyridin-2-ylmethyl)methaneamine for photocatalytic H_2 evolution behavior. They observed both in Cu(II) complexes [Cu(TMPA)Cl]Cl (**12**) and [Cu(Cl-TMPA)Cl$_2$] (**13**) that (**13**) is far efficient for photocatalytic H_2 production than (**12**), due to the presence of more labile Cl ligand with longer Cu-Cl bond length and a dangling Cl-substituted pyridyl unit in the second coordination sphere, which both contribute to a higher photocatalytic activity of complex (**13**). TMPA acts as a tetradentate ligand and coordinate with Cu(II) in a distorted trigonal manner; Cl-TMPA acts as a tridentate ligand coordinate to Cu(II) with two chloride ions in a distorted square pyramidal manner, leaving one Cl-substituted pyridyl group in the second coordination sphere structure which is given in **Table 1**. ESI-Ms data favor the formation of Cu-hydride intermediate for hydrogen evolution. The authors investigated the photocatalytic H_2 production activities in the presence of a multicomponent [Ir(ppy)$_2$(dtbpy)]Cl (ppy = 2-phenylpyridine, dtbpy = 4,4′-di-*tert*-butyl-2,2′-bipyridine) and triethylamine (TEA) photosystems as sacrificial reductant (SR) under optimal condition upon 6 h of irradiation of UV–visible light, the turnover number (TON) of which is calculated as 6108 for complex (**12**) and 10,014 for complex (**13**).

Based on the control potential electrolysis experimental data, the authors proposed photocatalytic hydrogen evolution mechanism. In the first step, excited PS system takes out one electron from TEA and donates to Cu^{II} center of complex (**13**). The protonated Cl-substituted pyridyl unit accepts that electron and kicks out the Cu-Cl center for the dissociation of Cl ligand which is substituted at the apical position which is more labile (longest bond length Cu-Cl). After that, the Cu^{I} species accept one e$^-$ and one H$^+$ from the reduced Cl-substituted pyridinium moiety; Cu^{II}-H center is formed as a key intermediate which lead to H_2 evolution. This executive mechanism provides us guidelines to design more efficient Cu-based catalysts for WRCs in the near future (**Figure 8**).

2.4 Ni electrocatalysts for HER

Professor Richard Eisenberg and coworker [77] synthesized a sequence of nickel bis(chelate) complexes; all complexes attained square planar geometry and examined photocatalytic as well as electrocatalytic behavior for hydrogen evolution.
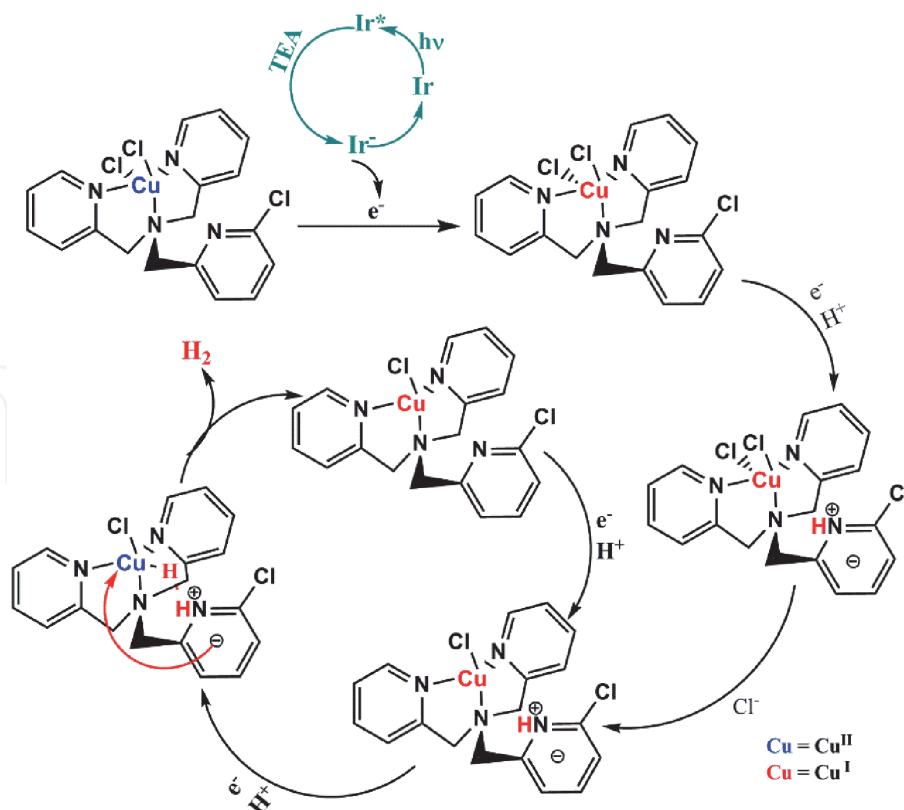
Figure 8.
Photocatalytic H$_2$ evolution mechanism for complex [Cu(Cl-TMPA)Cl$_2$] 12.

Fluorescein (Fl) as the photosensitizer along with triethanolamine (TEOA) as the sacrificial electron donor was used in water under basic medium (pH = 9.8). Bis (chelate) complexes (**14–17**) contain bdt(bisdithiolate) and their derivatives having S, O, or N as donors for coordination to the Ni center. The photochemical study reveals that only complexes **15** and **17** exhibited similar activity of hydrogen production in terms of TON (6000 mol of H$_2$ per mole of catalyst in 100 h). In contrast, the TON for the sample complex **16** was much lower ($\sim$900). Complex **14** was observed to be inactive for hydrogen generation. To understand the better significant result, the authors pursued electrochemical experiments under a fixed potential to examine the catalytic activity of complexes. In the absence of acid, both monoanionic complexes **14** and **17** exhibit only one reversible redox couple at -0.56 and -0.45 V, respectively, which is attributed to the [NiL$_2$]$^-$/[NiL$_2$]$^{2-}$ ligand-based reductions. The neutral complexes **15** and **16** exhibit two reversible reduction waves at -0.11 and -0.94 V and at -0.89 and -1.53 V, respectively. However, on increasing the concentration of acetic acid to these solutions, more negative catalytic waves were observed in cyclic voltammetry study. Complex **14** shows much more negative reduction potential (-2.25) which suggested this system is inactive for H$_2$ generation (as we discussed earlier). As is the case for complex **14**, **complex 16** exhibits a catalytic wave potential at -2.03 V which showed poor activity for H$_2$ generation as a consequence of not favorable electron transfer step from Fl$^-$ to the catalyst. Moreover, complexes **15** and **17** show activity for light-driven H$_2$ generation; these two complexes display electrocatalytic wave potential at significantly less negative at -1.64 and -1.62 V, respectively.

3. Concluding remarks and future scope

Here we present a recent development of molecular catalysts toward clean and renewable fuels using earth-abundant metals. We have highlighted a series of Co-,

Ni-, Cu-, Zn-based complexes for HER. We have recapitulated the fundamental principles of hydrogen and oxygen evolution reactions with molecular complexes. The designing and fabrication of the molecular complexes with redox-active ligands have been discussed in details; HER activity of the complexes strongly dependent on redox-active ligands as well the central metal ions are discussed in detail. A mechanistic approach and transfer of electron and proton during the homogeneous electrocatalyst and photocatalysts cycle are given in point. Although reasonable progress has been made in the development of metal complexes based electrocatalysts and chromospheres for photocatalytic hydrogen production, still several issues exist which need further improvement: (i) some photocatalytic systems suffer from low activities and short life times which is manifested in the instability of catalytic systems and so concern on the systems with modest water splitting activity and poor stability of the complexes. (ii) most of the complexes are not soluble in water leading to the use of organic solvent or mixture of organic-water solvent. From the future prospective, it is required to develop redox-active ligands with substituted functional group to increase the solubility of complexes in water. More experimental, spectroscopic, magnetic, and theoretical investigations is still needed to be carried out in order to understand the ligand- and metal-centered electron transfer processes. (iii) In addition, the overpotential requirements for most of the organic ligands are still very high, a chelating ligands giving much lower thermodynamic potentials and much smaller oxidation potential that should be utilized in future. (iv) In the regard of future growth in this field, with the need to design molecular complexes that can be immobilized on the surface of the electrode, for this purpose addition of suitable functional group in the ligand is necessity. These complexes can also be supported by the development of surface of the solid photocatalyst, like TiO_2, $BiVO_4$, etc. to demonstrate efficient photoelectrochemical cell.

Acknowledgements

Author details

Shipra Sagar[1], Ravi K. Kanaparthi[2], Manish K. Tiwari[3] and Satyen Saha[3*]

1 Department of Chemistry, Central University of Jharkhand, Ranchi, India

2 Department of Chemistry, Central University of Kerala, Kerala, India

3 Department of Chemistry, Institute of Science, Banaras Hindu University, Varanasi, India

*Address all correspondence to: satyen.saha@gmail.com

IntechOpen

References

[1] Lewis NS, Nocera DG. Powering the planet: Chemical challenges in solar energy utilization. Proceedings of the National Academy of Sciences of the United States of America. 2006;**103**: 15729-15735

[2] Kim D, Sakimoto KK, Hong D, Yang P. Artificial photosynthesis for sustainable fuel and chemical production. Angewandte Chemie, International Edition. 2015;**54**: 3259-3266

[3] Esswein AJ, Nocera DG. Hydrogen production by molecular photocatalysis. Chemical Reviews. 2007;**107**:4022-4047

[4] Tollefson J. Green carbon as a bridge to renewable energy. Nature. 2010;**464**: 1262-1264

[5] Pagliaro M, Konstandopoulos AG, Ciriminna R, Palmisano G. Solar hydrogen: Fuel of the near future. Energy & Environmental Science. 2010;**3**:279-287

[6] Armaroli N, Balzani V. The hydrogen issue. ChemSusChem. 2011;**4**:21-36

[7] Nocera DG. Solar fuels and solar chemicals industry. Accounts of Chemical Research. 2017;**50**:616-619

[8] Stamenkovic VR, Strmcnik D, Lopes PP, Markovic NM. Energy and fuels from electrochemical interfaces. Nature Materials. 2017;**16**:57-69

[9] Hwang J, Rao RR, Giordano L, Katayama Y, Yu Y, Shao-Horn Y. Perovskites in catalysis and electrocatalysis. Science. 2017;**358**: 751-756

[10] Andreiadis ES, Chavarot-Kerlidou M, Fontecave M, Artero V. Artificial photosynthesis: From molecular catalysts for light-driven water splitting to photoelectrochemical cells.

Photochemistry and Photobiology. 2011; **87**:946-964

[11] Joya KS, Joya YF, Ocakoglu K, van de Krol R. Water-splitting catalysis and solar fuel devices: Artificial leaves on the move. Angewandte Chemie, International Edition. 2013;**52**: 10426-10437

[12] Berardi S, Drouet S, Francis L, Gimbert-Surinach C, Guttentag M, Richmond C, et al. Visible light driven water splitting in a molecular device with unprecedentedly high photocurrent density. Chemical Society Reviews. 2014;**43**:7501-7519

[13] Song W, Chen Z, Brennaman MK, Concepcion JJ, Patrocinio AOT, Iha NYM, et al. Making solar fuels by artificial photosynthesis. Pure and Applied Chemistry. 2011;**83**:749-768

[14] Gust D, Moore TA, Moore AL. Solar fuels via artificial photosynthesis. Accounts of Chemical Research. 2009; **42**:1890-1898

[15] Zou Z, Ye J, Sayama K, Arakawa H. Direct splitting of water under visible light irradiation with an oxide semiconductor photocatalyst. Nature. 2001;**414**:625-627

[16] Hara M, Kondo T, Komoda M, Ikeda S, Shinohara K, Tanaka A, et al. Cu$_2$O as a photocatalyst for overall water splitting under visible light irradiation. Chemical Communications. 1998;**3**:357-358

[17] Wang X, Xu Q, Li M, Shen S, Wang X, Wang Y, et al. Photocatalytic overall water splitting promoted by an α–β phase junction on Ga$_2$O$_3$. Angewandte Chemie, International Edition. 2012;**51**:13089-13092

[18] Liao L, Zhang Q, Su Z, Zhao Z, Wang Y, Li Y, et al. Efficient solar

water-splitting using a nanocrystalline Co-O photocatalyst. Nature Nanotechnology. 2014;**9**:69-73

[19] Balat M. Potential importance of hydrogen as a future solution to environmental and transportation problems. International Journal of Hydrogen Energy. 2008;**33**: 4013-4029

[20] Wang M, Wang Z, Gong X, Guo Z. The intensification technologies to water electrolysis for hydrogen production, a review. Renewable and Sustainable Energy Reviews. 2014;**29**: 573-588

[21] Xu Y, Kraft M, Xu R. Metal-free carbonaceous electrocatalysts and photocatalysts for water splitting. Chemical Society Reviews. 2016;**45**: 3039-3052

[22] Oshima T, Lu D, Ishitani O, Maeda K. Intercalation of highly dispersed metal nanoclusters into a layered metal oxide for photocatalytic overall water splitting. Angewandte Chemie, International Edition. 2015;**54**: 2698-2702

[23] Chen X, Shen S, Guo L, Mao SS. Semiconductor-based photocatalytic hydrogen generation. Chemical Reviews. 2010;**110**:6503-6570

[24] Rausch B, Symes MD, Chisholm G, Cronin L. Decoupled catalytic hydrogen evolution from a molecular metal oxide redox mediator in water splitting. Science. 2014;**345**:1326-1330

[25] Symes MD, Cronin L. Decoupling hydrogen and oxygen evolution during electrolytic water splitting using an electron-coupled-proton buffer. Nature Chemistry. 2013;**5**:403-409

[26] Rausch B, Symes MD, Cronin L. A bio-inspired, small molecule electron-coupled proton buffer for decoupling the half-reactions of electrolytic water splitting. Journal of the American Chemical Society. 2013; **135**:13656-13659

[27] Zou Z, Ye J, Sayama K, Arakawa H. Direct splitting of water under visible light irradiation with an oxide semiconductor photocatalyst. Nature. 2001;**414**:625-627

[28] Zhang P, Wang M, Li C, Li X, Dong J, Sun L. Photochemical H_2 production with noble-metal-free molecular devices comprising a porphyrin photosensitizer and a cobaloxime catalyst. Chemical Communications. 2010;**46**:8806-8809

[29] Bartelmess J, Weare WW, Sommer RD. Synthesis, characterization and structural investigation of novel *meso*-pyridyl BODIPY–cobaloxime complexes. Dalton Transactions. 2013; **42**:14883-14891

[30] Yuan YJ, Tu JR, Lu HW, Yu ZT, Fan XX, Zou ZG. Neutral nickel(II) phthalocyanine as a stable catalyst for visible-light-driven hydrogen evolution from water. Dalton Transactions. 2016; **45**:1359-1363

[31] Karunadasa HI, Chang CJ, Long JR. A molecular molybdenum-oxo catalyst for generating hydrogen from water. Nature. 2010;**464**:1329-1333

[32] Kok B, Forbush B, McGloin M. Cooperation of charges in photosynthetic O_2 evolution - I, a linear four step mechanism. Photochemistry and Photobiology. 1970; **11**:457-475

[33] Askerka M, Brudvig GW, Batista VS. The O_2-evolving complex of photosystem II: recent insights from quantum mechanics/molecular mechanics (QM/MM), extended x-ray absorption fine structure (EXAFS), and femtosecond x-ray crystallography data. Accounts of Chemical Research. 2017; **50**:41-48

[34] Morales-Guio CG, Stern L, Hu X. Nanostructured hydro treating catalysts for electrochemical hydrogen evolution. Chemical Society Reviews. 2014;**43**: 6555-6569

[35] Laursen AB, Patraju KR, Whitaker MJ, Retuerto M, Sarkar T, Yao N, et al. Nanocrystalline Ni_5P_4: A hydrogen evolution electrocatalyst of exceptional efficiency in both alkaline and acidic media. Energy & Environmental Science. 2015;**8**: 1027-1034

[36] Huang Z, Chen Z, Chen Z, Lv C, Meng H, Zhang C. $Ni_{12}P_5$ nanoparticles as an efficient catalyst for hydrogen generation via electrolysis and photoelectrolysis. ACS Nano. 2014;**8**: 8121-8129

[37] Feng L, Vrubel H, Bensimon M, Hu X. Easily-prepared dinickel phosphide (Ni_2P) nanoparticles as an efficient and robust electrocatalyst for hydrogen evolution. Physical Chemistry Chemical Physics. 2014;**16**: 5917-5921

[38] Li R, Li C. Chapter one-Photocatalytic water splitting on semiconductor-based Photocatalysts. Advances in Catalysis. 2017;**60**:1-57

[39] Vozniuk O, Tanchoux N, Millet JM, Albonetti S, Di Renzo F, Cavani F. Horizons in Sustainable Industrial Chemistry and Catalysis. Vol. 178. Elsevier; 2019. pp. 281-302

[40] Yuan Y-J, Yu Z-T, Chen D-Q, Zou Z-G. Metal-complex chromophores for solar hydrogen generation. Chemical Society Reviews. 2017;**46**:603-631

[41] Tschierlei S, Karnahl M, Presselt M, Dietzek B, Guthmuller J, González L, et al. Photochemical fate: The first step determines efficiency of H_2 formation with a supramolecular photocatalysts. Angewandte Chemie, International Edition. 2010;**49**:3981-3984

[42] Fukuzumi S, Kobayashi T, Suenobu T. Photocatalytic production of hydrogen by disproportionation of one-electron-reduced rhodium and iridium–ruthenium complexes in water. Angewandte Chemie, International Edition. 2011;**50**:728-731

[43] Stoll T, Gennari M, Fortage J, Castillo CE, Rebarz M, Sliwa M, et al. An efficient Ru(II) -Rh(III) -Ru(II) polypyridylphotocatalyst for visible-light-driven hydrogen production in aqueous solution. Angewandte Chemie, International Edition. 2014;**53**:1654-1658

[44] Khine Ma SS, Hisatomi T, Domen K. Hydrogen production by photoctalytic water splitting. Journal of Japan Petroleum Institute. 2013;**56**(5):280-287

[45] Adams RE, Grusenmeyer TA, Griffith AL, Schmehl RH. Transition metal hydride complexes as mechanistic models for proton reduction catalysis. Coordination Chemistry Reviews. 2018; **362**:44-53

[46] Berardi S, Drouet S, Franca L, Gimbert-Suriñach C, Guttentag M, Richmond C, et al. Molecular artificial photosynthesis. Chemical Society Reviews. 2014;**43**:7501-7519

[47] Robinson SJC, Heinekey DM. Hydride & dihydrogen complexes of earth abundant metals: Structure, reactivity, and applications to catalysis. Chemical Communications. 2017;**53**: 669-676

[48] Schilter D, Camara JM, Huynh MT, Hammes-Schiffer S, Rauchfuss TB. Hydrogenase enzymes and their synthetic models: The role of metal hydride. Chemical Reviews. 2016;**116**: 8693-8749

[49] Gärtner F, Sundararaju B, Surkus AE, Boddien A, Loges B, Junge H, et al. Light-driven hydrogen generation: Efficient iron-based water reduction catalysts. Angewandte

Chemie, International Edition. 2009;**48**: 9962-9965

[50] Hollmann D, Gärtner F, Ludwig R, Barsch E, Junge H, Blug M, et al. Insights into the mechanism of photocatalytic water reduction by DFT supported in situ EPR/Raman spectroscopy. Angewandte Chemie, International Edition. 2011;**50**:10246-10250

[51] Gärtner F, Boddien A, Barsch E, Fumino K, Losse S, Junge H, et al. Photocatalytic hydrogen generation from water with iron carbonyl phosphine complexes: Improved water reduction catalysts and mechanistic insights. Chemistry - A European Journal. 2011;**17**:6425-6436

[52] Gartner F, Cozzula D, Losse S, Boddien A, Anilkumar G, Junge H, et al. Synthesis, characterisation and application of iridium(III) photosensitisers for catalytic water reduction. Chemistry - A European Journal. 2011;**17**:6998-7006

[53] Yuan YJ, Yu ZT, Gao HL, Zou ZG, Zheng C, Huang W. Tricyclometalated iridium complexes as highly stable photosensitizers for light-induced hydrogen evolution. Chemistry - A European Journal. 2013;**19**:6340-6349

[54] Lazarides T, Delor M, Sazanovich IV, McCormick TM, Georgakaki I, Charalambidis G, et al. Coutsolelos, Photocatalytic hydrogen production from a noble metal free system based on a water soluble porphyrin derivative and acobaloxime catalyst. Chemical Communications. 2014;**50**:521-523

[55] Muckerman JT, Fujita E. Theoretical studies of the mechanism of catalytic hydrogen production by a cobaloxime. Chemical Communications. 2011;**47** (46):12456-12458

[56] Nazeeruddin MK, Diau EWG, Yeh CY, Zakeeruddin SM, Gratzel M. Porphyrin-sensitized solar cells with cobalt (II/III)-based redox electrolyte exceed 12 percent efficiency. Science. 2011;**334**:629-634

[57] Franco F, Cometto C, Nencini L, Barolo C, Sordello F, Minero C, et al. Local proton source in electrocatalytic CO_2 reduction with $[Mn(bpy-R) (CO)_3Br]$ complexes. Chemistry - A European Journal. 2017;**23**:4782-4793

[58] Luca OR, Crabtree RH. Redox active ligands in catalysis. Chemical Society Reviews. 2013;**42**:1440-1459

[59] Lyaskovskyy V, de Bruin B. Redox non-innocent ligands: Versatile new tools to control catalytic reactions. ACS Catalysis. 2012;**22**:270-279

[60] Thompson EJ, Berben LA. Electrocatalytic hydrogen production by an aluminium (III)complex: Ligand-based proton and electron transfer. Angewandte Chemie, International Edition. 2015;**54**:11642-11646

[61] Solis BH, Maher AG, Dogutan DK, Nocera DG, Hammes-Schiffer S. Nickel phlorin intermediate formed by proton-coupled electron transfer in hydrogen evolution mechanism. Proceedings of the National Academy of Sciences of the United States of America. 2015;**113**: 485-492

[62] Luo G-G, Zhang H-L, Tao Y-W, Wu Q-Y, Tian D, Zhang Q. Recent progress in ligand-centered homogeneous electrocatalysts for hydrogen evolution reaction. Inorganic Chemistry Frontiers. 2019;**6**:343-354

[63] Ran J, Zhang J, Yu J, Jaroniec M, Qiao SZ. Earth-abundant cocatalysts for semiconductor-based photocatalytic water splitting. Chemical Society Reviews. 2014;**43**:7787-7812

[64] Berardi S, Drouet S, Francas L, Gimbert-Surinach C, Guttentag M, Richmond C, et al. Molecular artificial

photosynthesis. Chemical Society Reviews. 2014;**43**:7501-7519

[65] Yoshida M, Ueno S, Okano Y, Usui A, Kobayashi A, Kato M. Photochemical hydrogen production from 3d transition-metal complexes bearing *o*-phenylenediamine ligands. Journal of Photochemistry and Photobiology A: Chemistry. 2015;**313**: 99-106

[66] Konno Y, Matsushita N. pH-dependent color-change behavior of bis (*o*-phenylenediamine) platinum(II) complex and pH-dependent redox of bis (*o*-semibenzoquinonediimine)platinum (II) complex. Chemical Society of Japan. 2006;**79**:1046-1053

[67] Matsumoto T, Chang HC, Wakizaka M, Ueno S, Kobayashi A, Nakayama A, et al. Nonprecious-metal-assisted photochemical hydrogen production from *ortho-* Phenylenediamine J. American Chemical Society. 2013;**135**:8646-8654

[68] Roberts GM, Williams CA, Young JD, Ullrich S, Paterson MJ, Stavros VG. Unraveling ultrafast dynamics in photoexcited aniline. Journal of the American Chemical Society. 2012;**134**:12578-12589

[69] Keffer N, Chavarot-Kerlidou M, Artero V. Hydrogen evolution catalyzed by cobaltdiimine-dioxime complexes Acc. Chemistry Research. 2015;**48**: 1286-1295

[70] Giorgetti M, Berrettoni M, Ascone I, Zamponi S, Seeber R, Marassi R. X-ray absorption spectroscopy study on the electrochemical reduction of Co((DO) (DOH) pn)Br$_2$. Electrochimica Acta. 2000;**45**:4475-4482

[71] Zhang P, Jacques PA, Chavarot-Kerlidou M, Wang M, Sun L, Fontecave M, et al. Phosphine coordination to a cobalt diimine–dioxime catalyst increases stability

during light-driven H$_2$ production. Inorganic Chemistry. 2012;**51**:2115-2120

[72] Haddad AZ, Garabato BD, Kozlowski PM, Buchanan RM, Grapperhaus CA. Beyond metal-hydrides: Non-transition-metal and metal-free ligand-centered electrocatalytic hydrogen evolution and hydrogen oxidation. Journal of the American Chemical Society. 2016;**138**: 7844-7847

[73] Stubbert BD, Peters JC, Gray HB. Journal of the American Chemical Society. 2011;**133**:18070-18073

[74] Haddad AZ, Cronin SP, Mashuta MS, Buchanan RM, Grapperhaus CA. Metal-assisted ligand centered electrocatalytic hydrogen evolution upon reduction of a bis (thiosemicarbazonato)Cu(II) complex. Inorganic Chemistry. 2017;**56**: 11254-11265

[75] Zhang P, Wang M, Yang Y, Yao T, Sun L. A molecular copper catalyst for electrochemical water reduction with a large hydrogen-generation rate constant in aqueous solution. Angewandte Chemie, International Edition. 2014; **53**(50):13806-13807

[76] Wang J, Li C, Zhou Q, Wang W, Hou Y, Zhang B, et al. Photocatalytic hydrogen evolution by Cu(II) complexes. Dalton Transactions. 2016; **45**:5439-5443

[77] Das A, Han Z, Brennessel WW, Holland PL, Eisenberg R. Nickel complexes for robust light-driven and electrocatalytic hydrogen production from water. ACS Catalysis. 2015;**5**: 1397-1406